Parabolic and Hermite Cubic Finite Elements: A Flexible Technique for Deformable Models

Persephoni Karaolani, G.D. Sullivan, K.D. Baker

Intelligent Systems Group
Department of Computer Science
University of Reading
Reading, RG6 2AX
P.Karaolani@reading.ac.uk

Deformable models of elastic structures have been proposed for use in image analysis. The models are based on a minimum energy principle which incorporates both image information and "high level" knowledge of the structures involved. This paper reports a further development of the Finite Element Method (FEM) for use in active contour models. It is shown that parabolic and cubic Finite Elements provide a versatile technique for implementing deformable models. The method is demonstrated on MR and x-ray images of brain sections.

1. INTRODUCTION

In a previous paper [1] a modification to FEM, using parabolic elements, was reported. The method was demonstrated on "synthetic" arteries and its computational advantages were discussed. In this paper the parabolic elements are applied to the detection of structures in real images.

Hermite Cubic Finite Elements, which permit more complicated models to be used, are also reported. These offer faster and more stable convergence to the outline of an image structure under examination.

FEM in active contours

Models allow the use of high-level knowledge about expected structures to control the visual interpretation process. Most work on model-based vision has considered rigid [2] or parametrized [3] models. Recently, deformable models have also attracted attention, e.g. [4,5,6,7]. Deformable models are likely to have particular relevance in medical imaging applications, as a means of encoding the shapes of anatomical organs, which are inherently variable.

It is shown here that **parabolic and cubic Finite Elements**, provide a versatile technique for implementing deformable models. The models are based on a minimum energy principle which incorporates both image information and "high level" knowledge of the structures involved.

As an example, consider magnetic resonance images of brain sections. In order to accurately detect the boundaries of certain brain structures, given imperfect image data as derived from low level image techniques, it is useful to employ a model of the known "ideal" structure. A "stiff wire" can often serve as such a model. This model can be specified by minimising an energy integral, expressing the potential energy of the "wire".The model is thus a *variational model* as opposed to a geometrical one.

One method for minimising such an integral is based on the use of the Euler-Lagrange Theory (**ELT**) [4,5,6,7,8]. An alternative method is the Finite Element Method (**FEM**) which has been extensively used in computational studies of elasticity in structural mechanics. It offers many benefits over the more traditional ELT which has now been largely superseded.

In section 2 a description of the variational model in use is given. Section 3 offers an outline of the method. Also the benefit of Hermite cubic Finite Elements are stated. In section 4 a demonstration of the method in detecting brain structures is given and a slightly modified energy integral, used as a deformable model, is discussed.

2. DESCRIPTION OF THE MODEL

The "stiff wire" model is given by the function v(s) that minimises the integral in Eq. (1)

$$J(v(s)) = \int_0^L \left(\alpha \left| \frac{dv}{ds} \right|^2 + \beta \left| \frac{d^2v}{ds} \right|^2 + \gamma\, I(s) \right) ds \qquad (1)$$

The energy integral J(v(s)) is called a *functional* since its independent variable is a function.

- L is the domain of the parameter s (length of the "wire" model).

v(s) = ((x(s),y(s)) is the position vector on the image in terms of a parameter s over functions v(s).

- $|v|^2 = (x^2+y^2)$ is the Euclidean norm.
- The term $\alpha|v'|^2 + \beta\,|v''|^2$ represents the elastic energy stored in the wire
- I(v(s)) is the image intensity, or a function of the intensity, which acts as an external force deflecting the model towards the desired configuration.
- The parameters α, β, and γ are weights which can adjust the relative importance of the terms in Eq. (1).

If $\alpha > 0$, $\beta = 0$, the model describes a light elastic string.

If $\alpha = 0$, $\beta > 0$ the model acts like a very stiff thin beam.

Elastic strings are capable of deforming around sharp corners, whereas thin beams can only sustain smooth deflections. Thus by choosing α and β appropriately we can adjust the smoothness of the model.

BMVC 1990 doi:10.5244/C.4.58

The final term, I(v(s)), is used to allow chosen features of the image intensity values to influence the model. In the present treatment we use the image grey-values along v(s). I(v(s)) is given a positive sign if the model seeks dark areas (low intensity values) or a negative sign is used, if bright areas (maxima of intensity) are pursued.

3.PARABOLIC AND CUBIC FINITE ELEMENTS

FEM attempts to find an approximate solution to the minimum of J(v(s)). It works by converting the problem from one that seeks minima of functionals to one that approximates minima of ordinary functions of several independent variables.

In a diagrammatic form

$$\min_{v} J(v) \rightarrow \min_{v_j} J(v_j) \qquad (2)$$

where v_j are parameters to be determined, over predefined points v_j on the s axis.

A general description of FEM is given in [1], where its advantages for modelling deformable models, for model-based vision purposes are analysed. Briefly stated, the FEM approximates the unknown function v(s) over each element[1] by the expression:

$$v(s) \approx \hat{v}(s) = \sum_{j=1}^{N} v_j \, \phi_j(s) \qquad (3)$$

where ϕ_j are known Finite-Element basis functions and v_j are parameters to be determined from minimising $J(\bar{v}(s))$. Thus $J(\bar{v}(s))$ is a function over each element, of only N parameters v_j.

The type of element basis functions determines the value of N.

Parabolic elements correspond to N = 3. Parabolic elements can only approximate the "elastic string" model, i.e. they can minimise (2.1) for $\beta = 0$ This case was discussed in [1].

Hermite Cubic Finite Elements

In the case that $\beta \neq 0$ (Eq. 2.1), the theory of Finite Elements [9] do not permit the use of Parabolic Finite Elements. Iinstead Hermite cubic elements must be considered to model the term $\beta |v''|^2$.

Hermite cubics have continuous first derivatives and correspond to N = 4. The positional vector v over each element is given by:

$$v(s) \cong \hat{v}(s) = \sum_{1}^{2} (v_j \phi_j(s) + v'_j \psi'_j(s)),$$

where v_j are the deflections at node j, and v'_j is the tangent vector at node j.

Hermite Cubic Elements versus Parabolic Elements

• Parabolic Elements can be used only for "elastic string" models. Cubic elements permit the approximation of more complicated models, such as models with "stiff beam" properties.

• Hermite cubic elements have the property that the first derivative is continuous everywhere, and hence even in the case $\beta = 0$, they allow smoother solution than parabolic elements. Thus when sharp corners are modelled parabolic elements should be used.

• Hermite cubics are higher order (N = 4) elements than parabolics (N = 3). They thus give a better approximation to the exact solution of the minimum of the energy integral and obtain better convergence for the non-linear system of equations, resulting from the application of FEM. Higher order elements capture better the discontinuities in the external forces [9], represented here by the intensity values. Thus Cubic elements are better suited for modelling purposes in vision.

[1] The word element is used to denote a subdomain of the interval [0, L].

4. DEMONSTRATION OF HIGHER ORDER ELEMENTS.

The demonstrations that follow, employ Hermite cubic Finite Elements which show superior performance. Parabolic elements are used only in the artery demonstration for comparison. For convenience, the general term FEM will be used in this section to denote the Hermite Cubic Finite Elements.

Demonstrations of the "stiff wire" model, as approximated by FEM, are given for the detection of arteries in **x-ray** images and for the detection of boundaries of brain structures in Magnetic Resonance (**MR**) images of brain sections.

Due to the non-linear terms in Eq. (1), which describes the "wire" model, FEM leads to a non-linear system of equations that has to be solved with a numerical technique. The Euler time-step method is employed here.

The weights α, β, and γ are set an initial value. After a certain number of iterations the parameter β is lessened in order to allow the wire to settle in the minima or maxima of intensity values (section 2).

4.1 CT slices

In the CT slices the configuration of arteries is sought. A Gaussian of $\sigma = 1.5$ has been used to reduce the noise. The position of the arteries, shown as black or dark gray ribons in Figure 2, are represented by areas where there is a dip in intensity values. Thus minima of intensity values are sought and hence $\gamma > 0$ (Eq. (2.1)).

4.2 MR slices

In the MR images the task of detecting boundaries of different tissue type structures has been set. Each tissue type has an almost invariant grey level value.

The images have been blurred to reduce the noise, and differentiated so that maxima of intensity values occur where there is a difference in tissue type, i.e. where a boundary between certain structures appears. In this case $\gamma < 0$.

4.3Problems encountered in MR slices.

4.3.1 Partial Volume Effect

The thickness of the magnetic resonance slice (about 8 mm) gives rise to partial volume effects. This creates multiple step

edges instead of a single one on the area of the structure's boundary. When these edges are differentiated they give rise to multiple maxima.

This causes the wire model to proceed further in the interior of the boundaries where it settles in "satisfactory" maxima (Figure 1(f)).

4.3.1 Clusters

Bright areas occur further inside the boundaries of the ventricle's posterior horns (Figure 1(f)). These areas act as "attractors" for the model creating clusters of points. To avoid these clusters the penalty function given in Eq. (4) is employed.

4.4 Penalty function

A modification of Eq. (1) can be used in order to prevent cluster formation. This involves the addition of a penalty term to Eq. (1) given by:

$$PEN\left(\sum_j \left((x_j - x_{j+1})^2 + (y_j - y_{j+1})^2 + \delta\right)^{-1}\right) \quad (4)$$

where PEN is a weight controlling the importance of this term over the energy integral, and δ is a small number, introduced to prevent division with 0 when $x_j = x_{j+1}$ and $y_j = y_{j+1}$

Extra care has to be taken when using the penalty function. This is due to the instability that (4) brings to the non-linear system of equations.

ACTIVE CONTOURS VERSUS EDGE DETECTION TECNIQUES

Active contours have very desirable properties, especially for interactive segmentation of images. Medical images commonly have poor signal to noise ratios, and are often used to investigate anatomical structures that have poor contrast in the image. Manual intervention by highly skilled personnel using a pointing device is frequently used to identify and delineate anatomical structures; tools to assist the process are needed.

Conventional edge-tracing techniques have limited utility in low-contrast conditions. Edge-detectors such as the Marr-Hildreth [10] or the Canny[11, 12]operator initially classify individual pixels as "edgels", according to a strictly local property of the image distribution. Edgels are then typically grouped into connected strings, according to a strictly local definition of connectivity. This phase of the edge-description process represents a major problem in practical systems. The Canny operator fails to produce connected strings at T-junctions (Du Li 1989, [13]). The Marr-Hildreth operator is guaranteed to produce closed connected curves, but in low-contrast conditions this is often done at the expense of following random paths through noise.

Deformable models automatically lead to connected sequences, and help to simplify any poorly defined areas, by imposing a predefined structure. They adopt a final position which is the globally optimal solution (in the sense defined by the deformation forces and the initial conditions).

Demonstrations on MR slices of brain

Figure 1(a) shows part of an MR image of a brain section. The result of applying the Canny operator is shown in Figure 1(b & c). Thresholds in the connect algorithm were adjusted so that the ventricles (lower part of figure) stood out to the eye in Figure 1(b) and the head of the caudate nucleus (upper part of figure) was best visible in Figure 1(c). There is clearly a great deal more clutter in the latter, and both edge maps show many discontinuities.

Figure 1(d) shows the positions adopted by the FEM snakes, superimposed on the connect algorithm output shown in Figure 1(c), both using the same smoothed modulus of gradient image. In all cases the snake was initially looped very approximately around the structures by eye, with fixed points at the ends only (Figure 1(e)), and then allowed to contract under the elastic forces until it stabilised in the gradient image (Figure 1(f)). The smoothing and connecting properties of deformable models is evident.

In Figure 1(f) the "active contour's" position is further inside the outer boundary of the posterior horns of the lateral ventricle. The "contour" prefers to settle there instead of settling on the "edges" of the above mentioned structures, even though these two positions have similar intensity profiles. This is due to the fact that the elastic and stiffness energy are smaller on the settled position

Demonstration on CT images of brain arteries

Hermite Cubic Finite Elements not only give a smoother final configuration (Figure 2(b)) but also arrive at the final position in far less number of iterations than Parabolic Elements (Figure 2(c))

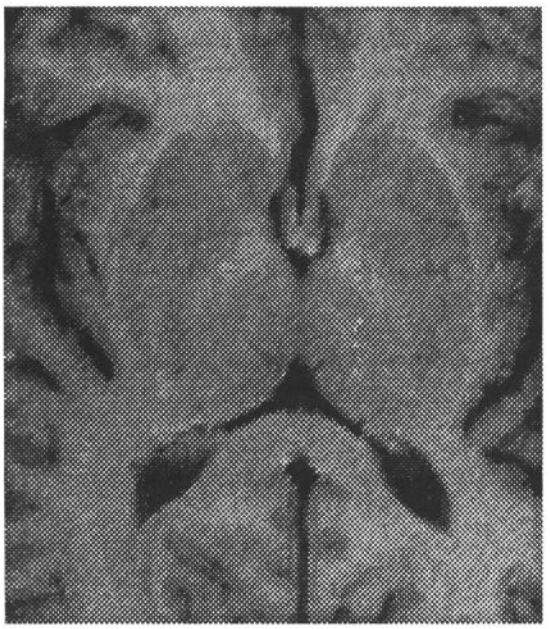

Figure 1a. MR image of brain section

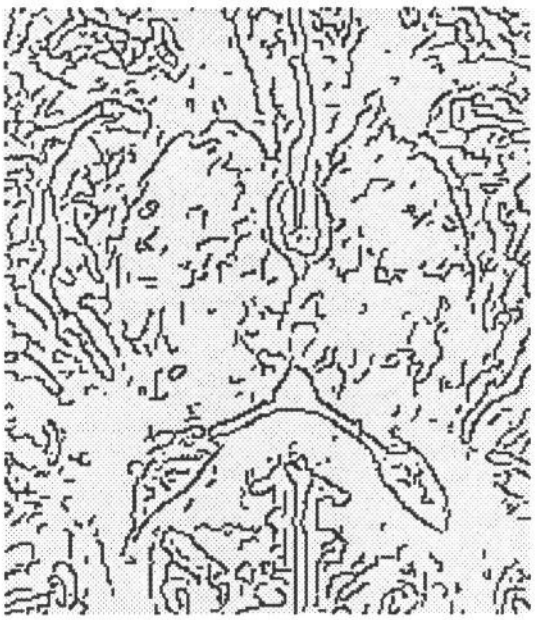

Figure 1c. Canny edges, using law thresholds for the connect

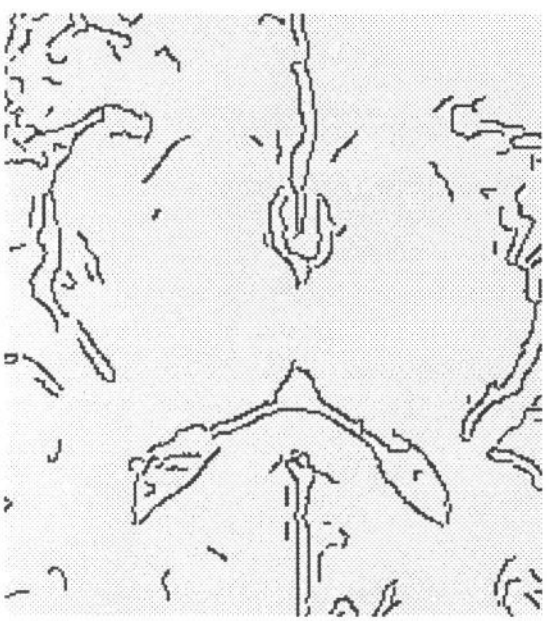

Figure 1b. Canny edges, using high thresholds for the connect phase

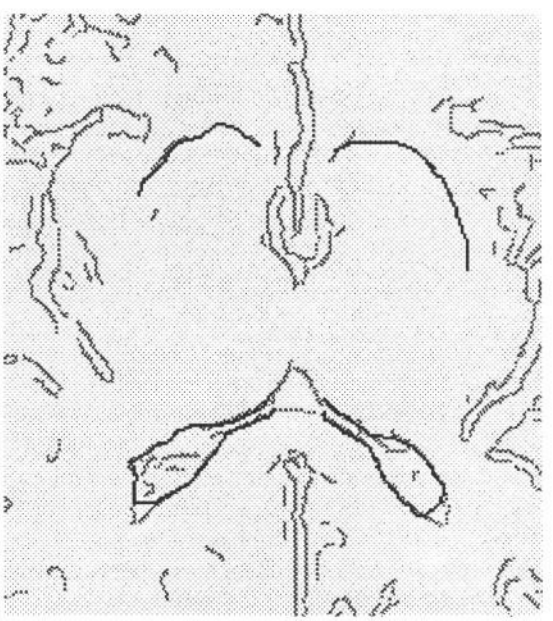

Figure 1d. Settled configuration of snakes superimposed on connected

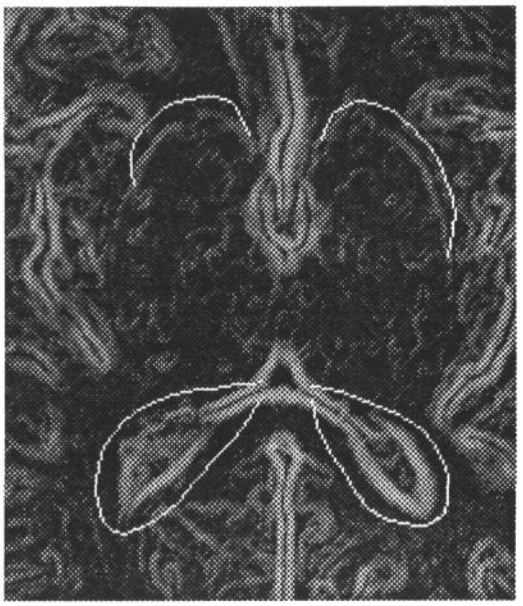

Figure 1e. Initial configuration of snakes on the gradient image

Figure 1f. Stable configuration of snakes

Figure 1(a-f). A comparison between the Canny edge detector and the snake algorith in an MR image

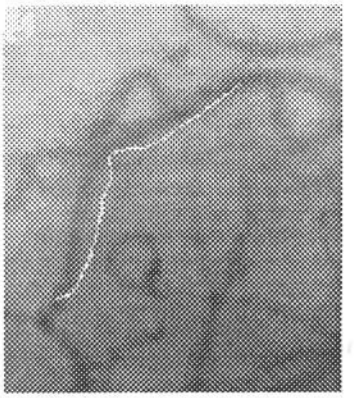

Figure 2a. Initial position

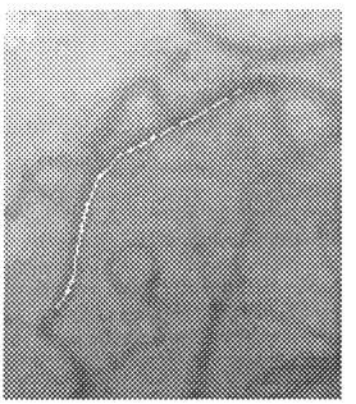

Figure 2b. Final position (Hermite Cubic Elements)

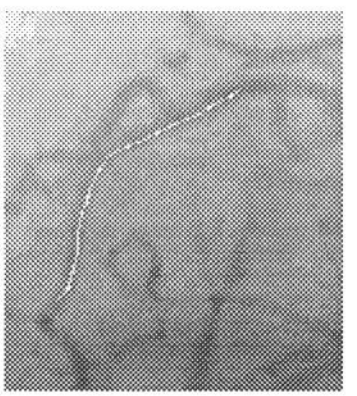

Figure 2c. Final position (Parabolic Elements)

Figure 2(a-c). Comparison between hermite cubic and parabolic FEM, inan x-ray image

References:

1. **Karaolani, P., Sullivan, G. D., Baker, K.D., Baines, M. J.** A Finite Element Method for Deformable Models, *Proceedings of the fifth Alvey Vision Conference*, (1989)
2. **Roberts., L.G.** Machine Perception of 3-d solids. In: Optical and Electro-optical Information Processing, J.P. Tippett, et al (Eds), MIT Press. 1965.
3. **Brooks, R.A.** Symbolic Reasoning among 3-d Models and 2-d Images. Stanford AI-Lab Memo AIM343, 1981.
4. **Kass, M., Witkin, A.,and Terzopoulos D.** Snakes: Active Contour Models, *Int. J. Computer Vision* 1. 321 - 331, 1987.
5. **Terzopoulos, D., Witkin, A. and Kass, M.** Symmetry-seeking models and 3D object reconstruction, *Int. J. Comp Vis.* **1**, 211-221. 1987.
6. **Terzopoulos D., Witkin A., Kass M.** Constraints on Deformable Models: Recovering 3D shape and Nonrigid Motion. AI, **36**, 91-123, 1988.
7. **Terzopoulos, D., Fleischer, K.** Deformable models, *Visual Computer* 4, 306 - 331, 1988
8. **Arthurs, A.M.**: Complementary Variational Principles, Oxford Math. Monographs, 1970
9. **Burnett, D. S.** Finite Element Analysis, Addison Wesley, 1987
10. **Marr, D.C., Hildreth, E.** Theory of edge detection, *Proc. Roy. Soc. London*, vol. B 207, pp. 187-217, 1980
11. **Canny, J.** Finding Edges and Lines in Images, Report AI-TR-720, Artificial Intelligence Laboratory, Massachusetts, 1983
12. **Canny, J.** A Computational Approach to Edge Detection, *IEEE PAMI* , vol. 8, No. 1, pp679-698,1986
13. **Li Du, Sullivan G. D., Baker K.D.** Edge Detection at Junctions, *Proceedings of the fifth Alvey Vision Conference*, 1989